Multiple functional therapeutic effects of the estrogen receptor β agonist indazole-Cl in a mouse model of multiple sclerosis

Spencer M. Moore[a], Anna J. Khalaj[a,b], Shalini Kumar[c], Zachary Winchester[a,b], JaeHee Yoon[a], Timothy Yoo[a], Leonardo Martinez-Torres[a,b], Norio Yasui[d], John A. Katzenellenbogen[d], and Seema Kaushalya Tiwari-Woodruff[a,b,c,e,1]

[b]Division of Biomedical Sciences at the School of Medicine, University of California, Riverside, CA 92521; [a]Department of Neurology, [e]Brain Research Institute, and [c]Intellectual and Developmental Disabilities Research Center, Semel Institute for Neuroscience at the School of Medicine, University of California, Los Angeles, CA 90095; and [d]Department of Chemistry, University of Illinois at Urbana–Champaign, Urbana, IL 61801

Currently available immunomodulatory therapies do not stop the pathogenesis underlying multiple sclerosis (MS) and are only partially effective in preventing the onset of permanent disability in patients with MS. Identifying a drug that stimulates endogenous remyelination and/or minimizes axonal degeneration would reduce the rate and degree of disease progression. Here, the effects of the highly selective estrogen receptor (ER) β agonist indazole chloride (Ind-Cl) on functional remyelination in chronic experimental autoimmune encephalomyelitis (EAE) mice were investigated by assessing pathologic, functional, and behavioral consequences of both prophylactic and therapeutic (peak EAE) treatment with Ind-Cl. Peripheral cytokines from autoantigen-stimulated splenocytes were measured, and central nervous system infiltration by immune cells, axon health, and myelination were assessed by immunohistochemistry and electron microscopy. Therapeutic Ind-Cl improved clinical disease and rotorod performance and also decreased peripheral Th1 cytokines and reactive astrocytes, activated microglia, and T cells in brains of EAE mice. Increased callosal myelination and mature oligodendrocytes correlated with improved callosal conduction and refractoriness. Therapeutic Ind-Cl-induced remyelination was independent of its effects on the immune system, as Ind-Cl increased remyelination within the cuprizone diet-induced demyelinating model. We conclude that Ind-Cl is a refined pharmacologic agent capable of stimulating functionally relevant endogenous myelination, with important implications for progressive MS treatment.

remyelination | experimental autoimmune encephalomyelitis | cuprizone diet | motor deficit | PI3/Akt/mTOR

Multiple sclerosis (MS) is an autoimmune, demyelinating, and neurodegenerative disease of the central nervous system (CNS) that affects 2–2.5 million people worldwide. Currently approved MS drugs reduce relapse rates but fail to reverse or prevent neurodegeneration and disability progression. Disease-modifying drugs capable of restoring neuronal function via axon remyelination (RM) represent a major unmet goal for MS therapeutics.

Oligodendrocyte (OL) progenitor cells (OPCs) are responsible for remyelinating axons, make up at least 3% of all white matter cells, and are present in and around MS lesions; however, they remain largely quiescent in the adult CNS (1). Although endogenous RM can occur in patients with MS, as evidenced by shadow plaques, it is short-lived, incomplete, and relatively ineffective (2). Transition to progressive MS is characterized by increased axon loss, which correlates with RM failure (3). Hence, a treatment that stimulates endogenous OPCs to differentiate and remyelinate axons would reduce axon degeneration and restore neuronal function.

Experimental autoimmune encephalomyelitis (EAE) affords researchers an in-depth, mechanistic understanding of immune-mediated, demyelinating neurodegeneration and anti-inflammatory effects of currently approved MS drugs. Our work has demonstrated promising neuroprotective effects of the estrogen receptor (ER) β agonist 2,3-bis(4-hydroxyphenyl)propionitrile (DPN) (4, 5). Although DPN, acting through ERβ, has a desirable palliative effect

in EAE, it possesses only 70-fold binding selectivity for ERβ over ERα and lacks anti-inflammatory effects (6, 7). A more selective ERβ agonist capable of immunomodulation would be more efficacious in treating inflammatory demyelinating neurodegeneration.

The structurally unique ERβ ligand indazole chloride (Ind-Cl), based on a halogen-substituted phenyl-2H-indazole core, is a preclinical development candidate with a strong dossier, including in vitro pharmacology using rodent and human cells, selectivity and potency data, promising absorption-distribution-metabolism-excretion findings, and pharmacokinetic profiling that includes confirmation of brain penetrability (mouse brain/plasma: ~1.0) (7, 8). It is a highly ERβ-selective (>100-fold) small molecule agonist that is administered s.c. and can be developed for oral administration (7).

Here, we explored pathologic, functional, and behavioral consequences of prophylactic and therapeutic (after onset of peak EAE) Ind-Cl in chronic EAE mice. Importantly, our recent finding of Ind-Cl-induced RM was confirmed, using the chronic cuprizone (CPZ)-induced demyelinating model (9), supporting Ind-Cl's remyelinating capabilities independent of its effects on primary inflammation. Our results demonstrate that prophylactic and therapeutic Ind-Cl have significant beneficial effects in a murine model of progressive MS. Specifically, Ind-Cl attenuates

Significance

In the search for effective multiple sclerosis treatment, much effort has been invested in estrogens and estrogen receptor (ER) agonists because of their neuroprotective benefits. However, because estrogens can produce ERα-based feminizing effects and cancer, ERβ agonists represent more desirable therapeutic candidates. The structurally unique ERβ ligand indazole chloride (Ind-Cl), a halogen-substituted phenyl-2H-indazole core, is a preclinical development candidate with a strong dossier. Our results indicate that Ind-Cl is effective in functionally ameliorating disease even when treatment is initiated at peak experimental autoimmune encephalomyelitis clinical disease. Ind-Cl's immunomodulatory and direct remyelinating effects result in motor dysfunction amelioration. These findings support Ind-Cl's potential to provide unique therapeutic benefits to patients with multiple sclerosis, as well as patients affected by other demyelinating disorders.
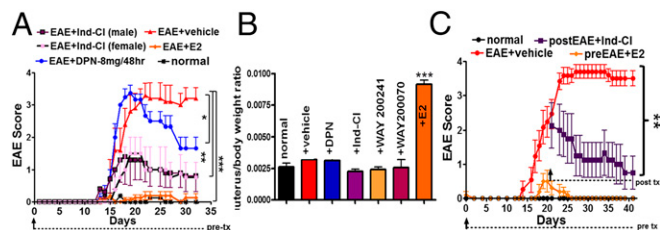
NEUROSCIENCE

Fig. 1. Prophylactic and therapeutic treatment with Ind-Cl decreases clinical scores, with no effect on uterine weight. (A) Mice were immunized with $MOG_{35–55}$. Normal mice did not receive $MOG_{35–55}$ or treatment. Treatments began on day 0 (prophylactic) until day 32. Vehicle-treated animals (red) displayed severe disease course beginning at ~day 15. E2 (0.04 mg/kg/d, orange) prevented the onset of clinical disease. In addition, 8 mg/kg/48 h DPN (blue) displayed decreased clinical scores over time, as observed previously (5). Ind-Cl (5 mg/kg/d) treatment in males (dark purple) and females (light purple) reduced clinical scores (A). One of three representative EAE experiments is shown. $n = 8$–10 mice/group. *$P < 0.05$, **$P < 0.01$, ***$P < 0.001$, ANOVA Friedman test. (B) Assessment of postperfusion uterus to body weight ratios from intact normal, EAE+vehicle, EAE+DPN (10 mg/kg/d), EAE+Ind-Cl (5 mg/kg/d), EAE+WAY 200241 (10 mg/kg/d), and EAE+WAY 200070 (10 mg/kg/d) and EAE+E2 (0.04 mg/kg/d) injected female mice revealed a fourfold increase in the E2-treated group and no differences between all other treatment groups ($n = 4$–5 mice/group; ***$P < 0.001$, ANOVA). (C) Mice were administered 5 mg/kg/d Ind-Cl therapeutically, beginning on day 21 (purple; postEAE), or 0.04 mg/kg/d E2 at day 0 (gold; preEAE) of active EAE or vehicle (red). EAE mice treated with Ind-Cl showed significant improvement. One of three representative EAE experiments is shown ($n = 10$ mice/group; **$P < 0.01$, ANOVA Friedman test). Reprinted from ref. 5 with permission from Elsevier (www.sciencedirect.com/science/journal/09699961).

clinical disease, and its functional immunomodulatory, remyelinating, and neuroprotective effects manifest in axon conduction and myelination improvements. Importantly, these effects correlate with improved motor function. Thus, Ind-Cl could impart much-needed, unique therapeutic benefits in progressive MS and other demyelinating disorders.

Results

Prophylactic Ind-Cl Decreases EAE Clinical Disease Severity Equally in Female and Male Mice.
Vehicle-treated EAE mice developed a persistent, chronic disease course starting at ~day 12–15. Female and male prophylactically Ind-Cl-treated (5 mg/kg) EAE mice showed attenuated clinical disease severity, with no sex difference in treatment response (Fig. 1A). Ind-Cl's effect was more pronounced than that of DPN, as DPN-treated female mice trended toward the same degree of clinical disease onset as vehicle-treated mice, but attenuated clinical disease after day 21–25 (4, 10). Ind-Cl reduced severity of peak clinical disease.

Ind-Cl During EAE Does not Increase Uterine Weight.
Estrogen augments uterine proliferative processes (11). Before detailed analyses, we assessed the effects of various ERβ ligands on body and uterine weight. Similar to observations with DPN (10), WAY 200070, WAY 200241, and Ind-Cl did not increase uterus/body weight, whereas E2 induced a fourfold increase (Fig. 1B).

Therapeutic Ind-Cl Attenuates EAE Clinical Disease Severity.
A therapeutic regimen (i.e., initiated after peak EAE disease) is most translationally relevant to MS treatment. Female mice were administered Ind-Cl beginning on day 18–21 (postEAE), when the mean clinical score was ~2.5. Control groups consisted of prophylactic E2-treated and vehicle-treated EAE mice (Fig. 1C). A significant decrease in body weight of EAE mice (12) treated with vehicle and Ind-Cl was observed, whereas prophylactic E2 treatment induced an increase compared with untreated normal control groups (Fig. S1). Therapeutic Ind-Cl attenuated a further increase in clinical scores. Importantly, therapeutic Ind-Cl-treated

mice exhibited a steady decline in clinical scores, reaching ~1.0 after 19–22 d of treatment.

Prophylactic and Therapeutic Ind-Cl Reduces Th1 Cytokine Production by Peripheral Immune Cells in EAE Mice.
To examine the mechanism of Ind-Cl effects on EAE, we evaluated peripheral immune response by measuring cytokine production from splenocytes. T-cell–secreted IFN-γ, IL-6, and proinflammatory IL-17 levels were comparable in vehicle-treated and prophylactic DPN-treated EAE animals but decreased with prophylactic Ind-Cl. Similarly, vehicle-treated and DPN-treated groups showed similar levels of macrophage-secreted TNF-α, which was reduced with Ind-Cl. Interestingly, IL-10, IL-13, and IL-5 levels were reduced only with prophylactic Ind-Cl. Overall, these results point to a profound immunomodulatory effect of Ind-Cl (*$P < 0.05$; Fig. 2A).

Prophylactic and Therapeutic Ind-Cl Reduces Immune Cells in EAE CNS.
Thoracic spinal cords of vehicle-treated EAE mice (day 36–40) displayed numerous multifocal to coalescing cell infiltrates (represented by $DAPI^+$ nuclei stain; Fig. 2 B, i). Prophylactic (day 0; preEAE) or therapeutic (day 21; postEAE/peakEAE) Ind-Cl reduced infiltrates. The majority of infiltrating cells were positive for pan-leukocyte marker $CD45^+$ microglia/macrophages and T cells ($CD3^+$). Glial fibrillary acidic protein (GFAP) and glutamine synthetase (GS)-positive astrocytes were also increased. Ind-Cl regimens reduced infiltrating $CD3^+$ and GS^+ cells and $CD45^+$ and $GFAP^+$ intensity in the dorsal column (DC) of EAE mice (Fig. 2B).
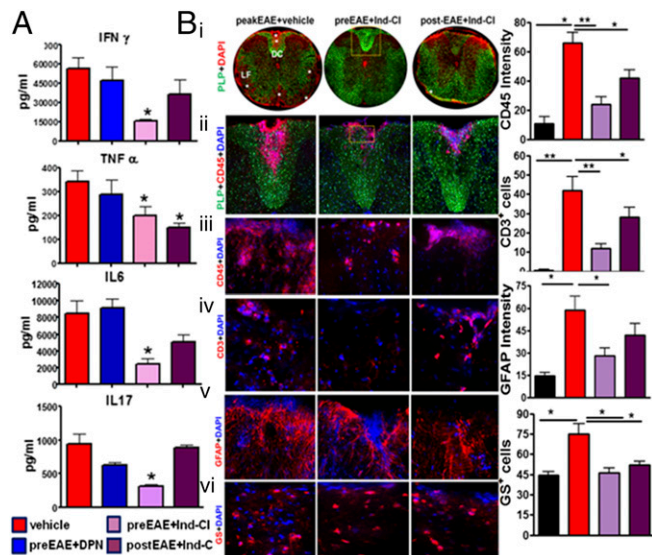

Fig. 2. Treatment with Ind-Cl suppresses cytokine production by peripheral immune cells and reduces CNS inflammation and infiltration. (A) Cytokine production by $MOG_{35–55}$-stimulated splenocytes was assessed from EAE mice killed on postinduction day 34. Pretreatment with DPN or Ind-Cl was initiated at day 0, and posttreatment with Ind-Cl began on day 21. DPN-treated (blue) and vehicle-treated (red) animals displayed similar cytokine levels. Pretreatment (light purple) with 5 mg/kg/d Ind-Cl resulted in significant reduction of all measured cytokines. Posttreatment with Ind-Cl (dark purple) significantly decreased TNFα levels. Data are representative of experiments repeated twice. $n = 4$–6 mice/group; *$P < 0.05$, t test. (B) CNS inflammation was assessed using immunohistochemistry. Asterisks within the representative 4× image of vehicle-treated EAE spinal cord indicate lesions and areas of infiltration and demyelination, unlike Ind-Cl-treated mice (i and ii). Ten times and 40× images of the DC (area delineated by the white dashed box) in i shows decreased infiltration by peripheral $CD45^+$ immune cells with Ind-Cl treatment (ii and iii) and decreased $CD3^+$ T-cell (red) numbers (iv). Pretreatment with Ind-Cl resulted in decreased $GFAP^+$ (red) intensity and GS+ (red) numbers, and a trend toward this effect was observed with posttreatment (v and vi). $n = 10$ mice/group; *$P < 0.05$, **$P < 0.01$, ANOVA.

Similar to previous observations, corpus callosum (CC) of EAE mice showed many periventricular infiltrating lesions around blood vessels and scattered throughout white matter, accompanied by microglia/macrophage and reactive astrocyte accumulation and fewer enhanced green fluorescent protein on the proteolipid promoter (PLP_EGFP$^+$) OLs (13, 14). EAE CC pathology resembles that observed in EAE DC. Ind-Cl decreased infiltrating immune cells and activated astrocytes in EAE CC (Fig. S2).

Ind-Cl Decreases and Restores Myelination in Spinal Cord and CC White Matter Tracts in EAE mice.

Our previous work reveals reduced axon numbers and myelination in the DC and CC by EAE day 21 (10, 13). Ind-Cl effects on axonal pathology and demyelination were evaluated. Similar to previous observations, vehicle-treated EAE mice showed decreased myelin (myelin basic protein, MBP$^+$) density (Fig. 3 I, A) in the DC and myelinated axons (MBP$^+$ and NF200$^+$) in the ventral column (Fig. 3 I, b). Contrastingly, Ind-Cl groups exhibited increased myelin density and myelinated axons (Fig. 3 I, a and b). Quantification of myelin density and NF200$^+$ staining revealed ∼50% (P < 0.001) reduction in vehicle-treated mice, whereas Ind-Cl-treated mice showed recovery of myelin density and myelinated axons (∼75% of normal controls; Fig. 3 I, c and d). Similarly, a decrease in MBP$^+$ CC intensity was observed in vehicle-treated mice (13) (Fig. 3 II, A). Ind-Cl treatment improved CC myelin intensity (Fig. 3 II, a and c).

To assess axon myelination integrity, ultrastructure EM analysis of the CC was performed. Mean ratio of inner axonal diameter to total outer diameter (g-ratio) for all myelinated and nonmyelinated axons within a given field (Fig. 3 II, b) was calculated. Out of all the callosal axons measured by EM, vehicle-treated mice showed increased numbers of nonmyelinated, 51 ± 4%, and thinly myelinated callosal fibers compared with only 8 ± 4% nonmyelinated axons in normal mice. Nonmyelinated axon numbers were decreased in Ind-Cl-treated CC: 18 ± 4% for preEAE+Ind-Cl and 22 ± 6% for postEAE+Ind-Cl. The mean g-ratio of vehicle-treated mice (0.91 ± 0.01) was higher than in normal mice (0.81 ± 0.01), whereas g-ratios of Ind-Cl-treated groups (preEAE+Ind-Cl, 0.75 ± 0.01; postEAE+Ind-Cl, 0.85 ± 0.005) and therapeutic DPN (0.85 ± 0.01) were lower than in the vehicle-treated group (**P < 0.01, ANOVA; Fig. 3 II, d).

Ind-Cl Increases Proliferating and Mature OL Survival.

To assess whether increased myelin intensity in Ind-Cl-treated EAE mice was a result of increased OPC survival, differentiation, and/or decreased OL apoptosis, CC cell populations were further analyzed. A direct comparison with normal CC revealed fewer PLP_EGFP$^+$ cells in vehicle-treated CC (Fig. 4 A and D). Meanwhile, Ind-Cl-treated CC revealed increased PLP_EGFP$^+$ cells. Morphological analysis of PLP_EGFP$^+$ cells showed improved cell soma and processes in Ind-Cl-treated EAE CC (Fig. 4 A and B). Because PLP_EGFP positivity does not distinguish between OPCs and OLs, consecutive brain sections were immunostained for OL transcription factor 2 (olig2) and mature OL marker adenomatous polyposis coli CC1. In Ind-Cl-treated EAE CC, an increase in OPCs was observed (Fig. 4 B and F). Moreover, CC1$^+$ OL numbers were improved in both Ind-Cl groups (*P < 0.05, ANOVA; Fig. 4 C and E).

A population of slowly dividing OPCs persists throughout the adult CNS (15), and OPCs can be generated from the subventricular zone (SVZ) in the adult rodent and human forebrain under physiological conditions and after demyelination (16). These OPCs are capable of proliferation, migration, differentiation, and axon RM (17); therefore, OPCs are attractive targets for therapeutic strategies. Because Ind-Cl during EAE increases OPC and mature OL numbers, we examined the SVZ (Fig. 4G). Vehicle-treated EAE SVZ exhibited fewer proliferating OPCs [colabeled with Ki67 (Fig. S3B) and olig2/platelet-derived growth factor α] compared with Ind-Cl-treated EAE SVZ. Similar increases in proliferating OPCs were observed in the spinal cord dorsal column (Fig. S3 A and C). Quantification of CC dorsally adjacent to SVZ indicated increased proliferating OPCs with therapeutic Ind-Cl (*P < 0.05, ANOVA; Fig. 4H).

Ind-Cl Increases OL Survival and Activates the PI3K/Akt/mTOR Pathway.

During EAE, many cell types (e.g., OLs) undergo apoptosis (5, 13, 18). Increased callosal OLs in Ind-Cl-treated EAE mice could be a result of decreased OL apoptosis and/or increased OL survival. Similar to previous observations, significant increases in caspase-3 activity were observed in vehicle-treated EAE groups (5), but not preEAE+ or postEAE+Ind-Cl− groups, via immunohistochemistry (Fig. S4). Overexpression of B-cell lymphoma 2 (BCl-2) is known to inhibit cell death. 2′,3′-Cyclic nucleotide-3′-phosphodiesterase (CNPase) is a myelin-associated enzyme expressed exclusively by differentiating OLs and makes up 4% of total CNS myelin protein. CNPase and BCl-2 levels were assessed in CC homogenates. During EAE, continued demyelination and cell death results in decreased CNPase and BCl-2 (Fig. 4 II, A and B). Therapeutic Ind-Cl increased CNPase and BCl-2 compared with vehicle-treated EAE and normal mice (*P < 0.05, **P < 0.01; Fig. S5 A and B).

To assess Ind-Cl effects on the potentially BDNF-mediated PI3K/Akt/mTOR pathway [also modulated by DPN (6, 19–21)] in EAE mice, CC homogenates were probed for relevant proteins
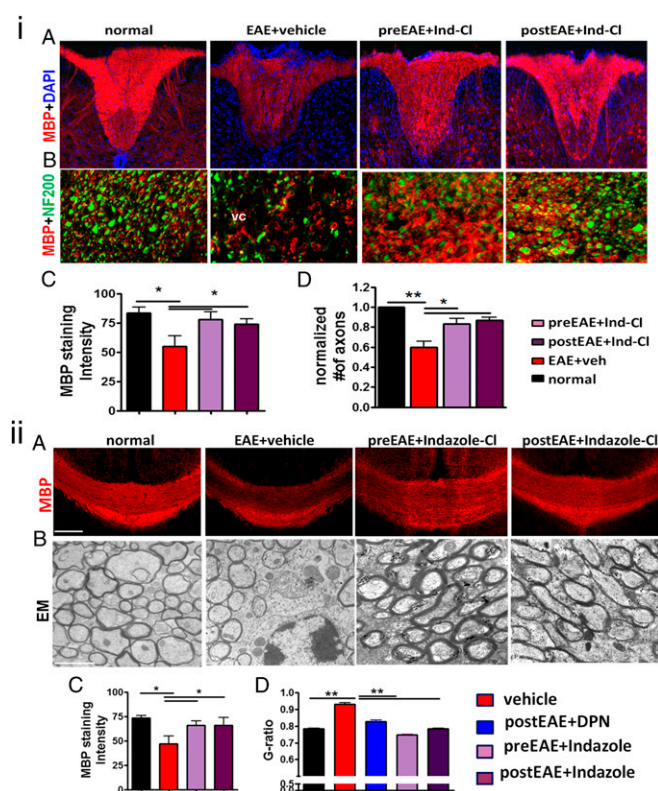

Fig. 3. Ind-Cl treatment improves myelination and myelinated axon numbers in the spinal cord and corpus callosum of EAE mice. (i) Myelination (A) and myelinated axon (B) levels were assessed by staining for myelin basic protein (myelin) and neurofilament 200 kDa (NF200; axons). Representative 10× magnification images of the dorsal column reveal increased MBP$^+$ intensity (red) with Ind-Cl pre- and posttreatment (A and C). Forty times magnification images of ventral column reveal an increased number of NF200$^+$ axons (green) surrounded by MBP$^+$ rings (red) with Ind-Cl pre- and posttreatment, indicating improved myelinated axon numbers (B and D). (ii) Myelination levels within the CC were examined via immunohistochemistry (A) and electron microscopy (B). Representative 10× magnification images of midline-crossing CC from coronal brain sections stained for MBP; red are shown (A). Both pre- and posttreatment with Ind-Cl improved MBP$^+$ intensity (A and C). Representative electron micrographs of CC axons imaged at 14,000× magnification (B) reveal lower g-ratios in all Ind-Cl-treated groups (D), representative of increased axon myelination. The Ind-Cl-treated EAE group had mean g-ratio comparable to that of the postEAE+DPN (positive control). A minimum of 500 axons were measured per mouse. (Scale bars, A, 100 μm; B, 1.0 μm.) n = 4–8 mice/group; *P < 0.05, **P < 0.01, ANOVA.
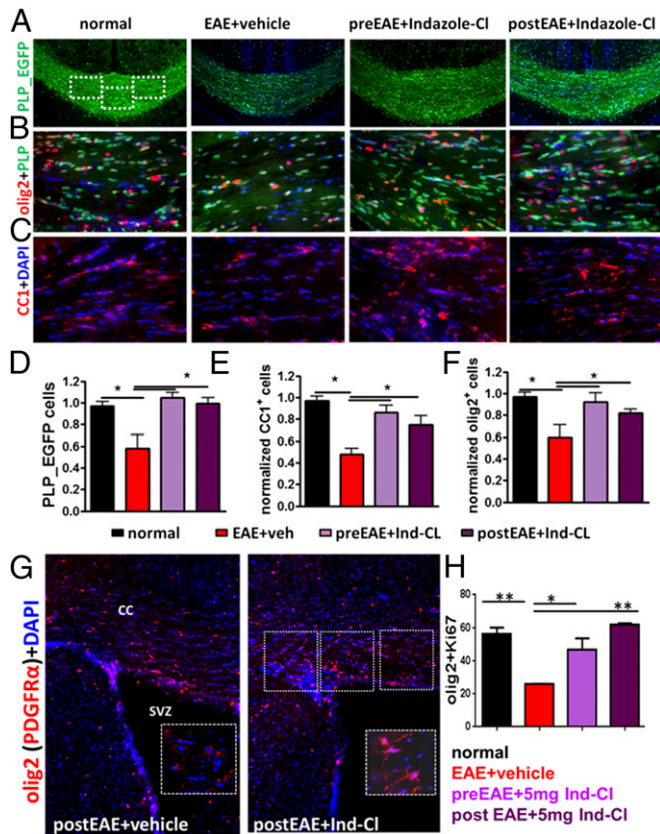
Fig. 4. Ind-Cl increases survival, proliferation, migration, and differentiation of OPC in the SVZ and CC of EAE mice. Improved PLP_EGFP[+] cell numbers in animals pre- and posttreated with Ind-Cl were observed (*A* and *D*). White dashed boxes within the normal CC (*A*) depict areas examined at 40× magnification in *B* and *C*. Ind-Cl treatment improved numbers of olig2 (red)-stained cells (*B* and *F*). Increase in adenomatous polyposis coli (CC1; red) immunostaining revealed improved mature OL numbers in all Ind-Cl-treated groups (*C* and *E*). Costaining with olig2 (red) and platelet-derived growth factor α (inset; red) was used to determine the percentage of OPCs (*G* and *H*). Representative 20× magnification images of coronal brain slices containing CC adjacent to the SVZ are shown, with the dashed box indicating the region imaged at 40× magnification and represented in the inset (*G*). Prophylactic or therapeutic Ind-Cl treatment increased the percentage of proliferating Ki67+ and olig2+ OPCs near-SVZ CC compared with the vehicle-treated group. n = 8 mice/group; *P < 0.05, **P < 0.01, ANOVA.

(6, 5). Therapeutic Ind-Cl increased BDNF and phosphorylated (p)-AKT and p-mTOR (*P < 0.05, **P < 0.01, Fig. S5 C and D).

Ind-Cl Improves Callosal Axon Conduction. To characterize the functional consequence of CC neuropathology during EAE and with Ind-Cl, callosal compound action potentials (CAPs) were recorded (Fig. 5 I, a). Typical voltage traces showing two downward phases of the N1 and N2 CAP amplitudes, likely representing fast depolarizing large, myelinated axons and slower depolarizing non-myelinated axons, respectively, are shown (13) (Fig. 5 I, a and b). During EAE (red), both N1 and N2 CAP amplitudes were decreased to nearly 50% of normal (black; Fig. 5 I, a and b). Prophylactic Ind-Cl (light purple) and DPN (navy) increased N1 and N2 CAP amplitudes compared with vehicle treatment. Therapeutic Ind-Cl (dark purple) induced an increase in N1, but not N2, CAP amplitude (Fig. 5 I, c and d; **P < 0.001, *P < 0.05).

To further investigate Ind-Cl effects on EAE-induced CC axon deficits, axon refractoriness was examined (9). In the normal group, the N1 component evoked by the second pair of pulses was 50% of the amplitude of a single pulse presentation at an interpulse interval (IPI) of 2.2 ± 0.1 ms (Fig. 5 I, e). The IPI for the vehicle-treated

EAE group had a slower response of 5.1 ± 0.2 ms. Prophylactic Ind-Cl and DPN, and therapeutic Ind-Cl, callosal axons had faster IPIs of 3.8 ± 0.1, 3.7 ± 0.2, and 3.7 ± 0.1 ms, respectively. The N2 component IPIs from vehicle-treated mice (8.8 ± 2.2 ms) were slower than those of normal mice (3.2 ± 0.2 ms). Ind-Cl induced a small but significant recovery: preEAE+Ind-Cl = 4 ± 0.2 ms, preEAE+DPN = 4.4 ± 0.2 ms, and postEAE+Ind-Cl = 4.7 ± 0.2 ms.

Therapeutic Ind-Cl Decreases EAE-Induced Rotorod Motor Performance Deficit. To assess the functional significance of Ind-Cl in vivo, EAE mice were tested for their ability to remain walking on a rotating cylinder. The rotorod task has strong translational correlates to motor assessments, using the Kurtzke Expanded Disability Status Scale, in patients with MS. EAE mice display an increased tendency to fall from the cylinder compared with normal mice, which are capable of remaining on the cylinder for the full trial period. At day 21, mice were randomly assigned to receive therapeutic vehicle or Ind-Cl (Fig. 5 II, a). Ind-Cl attenuated EAE clinical disease, whereas vehicle-treated mice displayed severe and chronic disability beginning at ~day 15 (Fig. 5 II, a). Rotorod performance declined sharply as clinical disability progressed, but Ind-Cl rescued motor function; Ind-Cl-treated mice approached normal performance levels within 10–12 d of treatment initiation (Fig. 5 II, a and b). By day 30–40, Ind-Cl-treated EAE mice exhibited recovery of motor function (**P < 0.01, ANOVA; Fig. 5 II, a and b).
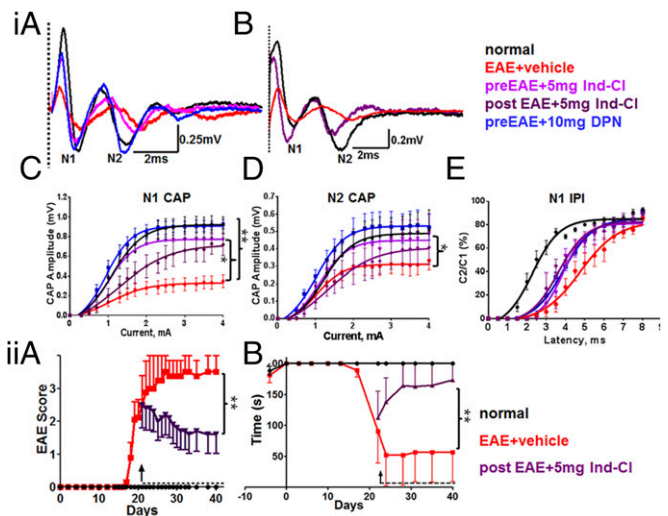

Fig. 5. Prophylactic and therapeutic treatment of EAE mice with Ind-Cl improves callosal conduction, axon refractoriness, and rotorod motor performance. (*i*) Callosal axon conduction and refractoriness of normal, vehicle-treated, Ind-Cl-treated, and DPN-treated EAE mice were evaluated. Treatments in *A* were initiated at postinduction day 0 (pretreatment) and on day 21 after EAE induction in *B* and continued until experiment end (day 32 or 40). Representative CAP recordings from both treatment group are shown in *a*. N1 (*C*) and N2 (*D*) CAP amplitudes of vehicle-treated EAE callosal axons (red) were significantly smaller than in normal controls (black). Similar to DPN (blue), Ind-Cl [light purple (preEAE) and dark purple (postEAE)] treatment resulted in near-normal N1 and N2 CAP amplitudes. In addition, Ind-Cl and DPN treatment produced a leftward shift in N1 IPI relative to the vehicle-treated group, indicating improved myelinated axon refractoriness (*E*). n = 8 mice/group; *P < 0.05, **P < 0.01, ANOVA. (*ii*) Ind-Cl-treated mice displayed decreased clinical scores (*A*) beginning ~5 d after treatment initiation and lasting throughout the observation period, indicative of reduced clinical disease severity. To assess motor function, mice were subjected to rotorod motor performance testing (*B*). Vehicle-treated EAE mice displayed an abrupt and consistent decrease in time (seconds) remaining on the rotorod. Ind-Cl treatment, EAE mice displayed an increase in time remaining on the rotorod, representative of improved motor function. Data are representative of experiments repeated three times. n = 10 mice/group; **P < 0.01, ANOVA.

Ind-Cl-Induced Axon RM Improvement Occurs Independent of Primary Inflammation Effects. In contrast to EAE, CPZ diet-induced demyelination does not compromise the blood–brain barrier and elicits no primary infiltrating autoimmune response. To examine the direct effects of Ind-Cl on RM/neuroprotection in the absence of its effects on primary inflammation, the CPZ diet model was used. Nine weeks of CPZ diet (9 wk CPZ) resulted in extensive demyelination and loss of PLP_EGFP^{+} cells throughout the cortical layers, CC, and dorsal hippocampus (Fig. 6A). Assessment of CC myelin and mature OLs revealed decreases in the 9-wk-DM group (9wk-DM). A subset of 9-wk-DM mice were switched to 3 wk of normal diet (ND) and underwent RM (9wkCPZ+3wkND), during which half were administered vehicle (+V) or Ind-Cl (+Ind-Cl). Both RM groups showed myelin density and mature OL recovery (Fig. 6B). Ind-Cl resulted in a ~30% increase in CC myelination and OLs compared with the vehicle-treated RM group. Direct positive effects of Ind-Cl on axon RM were confirmed by EM analysis, as Ind-Cl during RM resulted in a lower g-ratio compared with 9wk-DM alone and vehicle-treated 9wkCPZ+3wkND-RM groups (normal = 0.86 ± 0.01; 9wkCPZ = 0.96 ± 0.01; 9wkCPZ+3wkND+V = 0.94 ± 0.01; and 9wkCPZ+3wkND+Ind-Cl = 0.89 ± 0.003; *$P < 0.5$, **$P < 0.01$, ***$P < 0.001$, ANOVA; Fig. 6C).

Discussion

In MS, demyelinated areas containing damaged axons are associated with inflammatory reactions orchestrated by activated T cells, macrophages, and endogenous glia, which produce proinflammatory and neurotoxic factors and attenuate repair/RM of damaged/demyelinated axons (22). This manifests as clinical deficits (23, 24). Thus, these cell types are immunomodulation targets in MS. Currently approved immunomodulators are only modestly effective in reducing relapses by slowing disability accumulation; these treatments fail to stop axon loss and/or stimulate RM. OL and myelin rescue and sustenance, with immunomodulation, are of high priority for effective MS therapy development.

In the search for effective MS treatments, much has been invested in estrogens and ER agonists because of their neuroprotective benefits (5, 10, 25, 26). Different ERβ ligand analogs have distinct effects on gene transcription in signaling pathways for chromosome replication, cell death, and OPC differentiation (27). The therapeutic potential of ERβ-selective compounds is particularly favorable because beneficial effects of ERβ activation are independent of undesired proliferative effects on breast and uterine tissue, which are principally ERα-mediated (28). Certain haloindazoles, synthetic ERβ-specific ligands based on a halogen-substituted phenyl-2H-indazole core (8), potently inhibit transcriptional activation of inflammatory response genes in microglia and astrocytes (7). Our study demonstrates that the haloindazole Ind-Cl ameliorates chronic EAE even when treatment is initiated at peak clinical disease. We analyzed callosal white matter integrity in addition to spinal cord, as MS CC reflects demyelinating lesions, diffuse tissue damage, and neural connectivity abnormalities (29, 30). Specifically, Ind-Cl inhibits ongoing demyelination and axon damage in EAE, leading to substantial recovery of axon conduction, a functional indicator of axon myelination and neuroprotection. Ind-Cl increased BDNF, decreased cell death markers, and activated the PI3K/Akt/mTOR signaling pathway required for OPC proliferation and OL differentiation. Furthermore, therapeutic Ind-Cl reversed ongoing motor deficit. In contrast to DPN's effects, the present study confirms a reduction of reactive astrocytes by Ind-Cl. Reactive astrocytes respond to and magnify ongoing inflammatory response. We report that both EAE-induced peripheral immune response and CNS immune cell increases are reduced with prophylactic Ind-Cl, which is further evidence of this drug's promising immunomodulatory properties.

ER β is present in various cell types within the peripheral immune system and CNS, including neurons, astrocytes, microglia, OLs, and immune cells (31). Using conditional gene knockout mice, we have shown that the functional beneficial effects of the less-selective ERβ agonist DPN in EAE mice are largely attributable to its action on ERβ in OL lineage cells (6). Further,
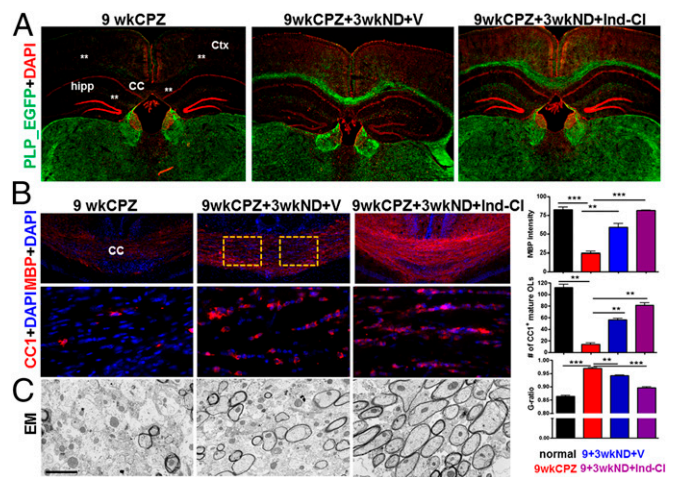

Fig. 6. Treatment with Ind-Cl improves RM in the CC of CPZ-induced demyelinated mice. (A) Coronal brain sections were stained with DAPI (red) and imaged at 2× magnification. Mice subjected to CPZ diet for 9 wk (9wkCPZ/DM) show significantly less PLP_EGFP fluorescence throughout the cerebral cortex layers, CC, and dorsal hippocampus, as indicated with white asterisks. A group of 9wkCPZ mice subsequently switched to normal diet and treated with vehicle for 3 wk (9wkCPZ+3wkND+V) showed recovery in PLP_EGFP fluorescence. The subset of mice treated with Ind-Cl during the RM period (9wkCPZ+3wkND+Ind-Cl) showed greater increases in PLP_EGFP fluorescence compared with mice in the vehicle-treated group. (B) Myelination levels and changes in mature OLs within the CC of these mice was assessed by immunostaining for MBP (red) and CC1 (red). Although MBP[+] intensity and CC1^{+} OL numbers were reduced in 9wkCPZ sections, Ind-Cl treatments induced a significantly greater recovery in myelin and mature OLs. (C) Representative electron micrographs of CC axons imaged at 14,000× magnification reveal significant axon demyelination of callosal axons. Ind-Cl treatment during the RM period significantly augmented axon myelination. A significant increase in g-ratio is evident in the 9wkCPZ group. Contrastingly, the 9wkCPZ+3wkND+Ind-Cl group's g-ratio was a significantly decreased compared with vehicle treatment alone. A minimum of 500 axons were measured per mouse. (Scale bar, C, 1.0 μm.) $n = 4–8$ mice/group; *$P < 0.05$, **$P < 0.01$, ***$P < 0.001$, ANOVA.

increased BDNF expression in DPN-administered mice lacking ERβ in OLs is not sufficient to reduce clinical disease or demyelination or to increase the PI3K/AKT/mTOR pathway activation, although it may explain partial improvement of axonal loss and conduction (5, 6). It would follow that the functional benefits of therapeutic Ind-Cl, a more selective ERβ agonist, are at least partly attributable to the drug's actions on ERβ in OL lineage cells. However, unlike DPN, Ind-Cl exhibits immunomodulatory capabilities in both the peripheral immune system and CNS (7). Ind-Cl may concurrently act on ERβ in multiple cell types. An effect of Ind-Cl on peripheral cells does not exclude a direct effect on the CNS. Time of treatment initiation may contribute to predominant Ind-Cl mechanism of action in EAE. For example, immunomodulatory capabilities may yield indirect neuroprotection (i.e., prevention of neurodegeneration caused by immunomodulatory response) if treatment is initiated early in disease, whereas treatment initiation late in disease may rely on the direct neuroprotective (i.e., restoration of neuronal components, including myelinating OLs, and function) capabilities of Ind-Cl, which we have demonstrated here in the CPZ diet-induced demyelination, a model with an intact blood–brain barrier and no primary inflammatory response.

The difference in immunomodulatory plus remyelinating properties of Ind-Cl and the solely remyelinating properties of DPN raises questions about ERβ binding affinity, selectivity, gene regulation, and mechanisms of action of various ERβ ligands. Thus, it is not surprising that structurally related ERβ ligands, even ones having similar ERβ versus ERα binding affinity, selectivity, and efficacy in standard reporter gene assays, have distinct patterns of endogenous gene regulation. In light of such findings, one may understand why the actions of Ind-Cl through ERβ are different

NEUROSCIENCE

(i.e., more favorable) in terms of amelioration and reversal of MS-like symptoms compared with DPN and other ERβ ligands (5, 7, 32). Furthermore, although estradiol is a more potent ligand for ERβ than Ind-Cl, it reverses some of the anti-inflammatory effects of Ind-Cl (7), so its therapeutic efficacy in MS (irrespective of increased risk of breast and uterine cancer) is questionable.

Ind-Cl's distinct immunomodulating and regenerative/remyelinating effects support its potential to provide unique therapeutic benefits to patients with secondary and progressive MS, as well as patients with other demyelinating disorders. Because MS is a multifocal disorder, systemic delivery of Ind-Cl, a brain-penetrable small-molecule compound, is expected to provide greater therapeutic benefit compared with other ER ligands and cell-based therapies.

Materials and Methods

Treatment. Ind-Cl [synthesized by J.A.K.'s laboratories (8)] was dissolved in 10% ethanol + 90% (vol/vol) Miglyol 812N (vehicle; Sasol) and administered s.c. daily at 5 mg/kg body weight. Control groups received (s.c.) either 0.04 mg/kg/d 17β-estradiol (E2) or 8 mg/kg/48 h DPN (4, 10). Treatment was initiated at EAE postinduction day 0 (preEAE) or day 21 (post/peakEAE) and continued until day 40. For CPZ experiments, animals received Ind-Cl or vehicle during RM only ($n = 10–15$ per group; two to three experiments).

EAE. Active EAE was induced in 8-wk-old male and female PLP_EGFP C57BL/6 mice (4, 10, 13). All procedures were conducted in accordance with the NIH and approved by the Animal Care and Use Committee at the University of California, Los Angeles,.

CPZ. Male PLP_EGFP mice were randomly assigned to one of two groups. The normal myelination group received normal chow. The demyelination group ($n = 32$) received 0.2% CPZ-milled chow for 9 wk (33). DM animals ($n = 10$) were killed, and the remaining 24 animals were returned to normal chow (RM), during which they received daily Ind-Cl or vehicle ($n = 12$ per group).

Rotorod. Each mouse was tested for motor function twice a week, using a rotorod (6).

Peripheral cytokines. Cytokine levels were assessed from $MOG_{35–55}$-stimulated splenocyte supernatant by Searchlight (Aushon Biosciences) (34).

Histopathology and immunohistochemistry. Formalin-fixed CNS sections were examined by immunohistochemistry (10). In parallel, CC was examined using EM (4).

Microscopy and quantification. Immunostaining was quantified using unbiased stereology (34). For EM, serial ultrathin sections of Epon-embedded CC stained with uranyl acetate-lead citrate were analyzed (4).

Electrophysiology. Coronal brain slices corresponding to plates 40–48 (35) were used for recordings (4, 9).

Western blot. Dissected CC (some cortex, no hippocampus) was rapidly frozen and stored at −80 °C. Polyacrylamide gel electrophoresis and immunoblotting were performed (5). Lanes represent individual animals (graphs, $n = 4–8$ animals per group over the course of two to three experiments).

Statistical analysis. Statistical analysis of mean values was carried out using one-way ANOVA or Friedman Test (for clinical scores), where *$P < 0.05$ was considered significant. Western blot data are presented as mean ± SEM and analyzed by t test for independent samples or two-way ANOVA. MicroCal Origin or Prism 4 (GraphPad Prism Software Inc.) were used.

1. Scolding N, et al. (1998) Oligodendrocyte progenitors are present in the normal adult human CNS and in the lesions of multiple sclerosis. *Brain* 121(Pt 12):2221–2228.
2. Smith KJ, McDonald WI (1999) The pathophysiology of multiple sclerosis: The mechanisms underlying the production of symptoms and the natural history of the disease. *Philos Trans R Soc Lond B Biol Sci* 354(1390):1649–1673.
3. Kornek B, et al. (2000) Multiple sclerosis and chronic autoimmune encephalomyelitis: A comparative quantitative study of axonal injury in active, inactive, and remyelinated lesions. *Am J Pathol* 157(1):267–276.
4. Crawford DK, et al. (2010) Oestrogen receptor beta ligand: A novel treatment to enhance endogenous functional remyelination. *Brain* 133(10):2999–3016.
5. Kumar S, et al. (2013) Estrogen receptor β ligand therapy activates PI3K/Akt/mTOR signaling in oligodendrocytes and promotes remyelination in a mouse model of multiple sclerosis. *Neurobiol Dis* 56:131–144.
6. Khalaj AJ, et al. (2013) Estrogen receptor (ER) β expression in oligodendrocytes is required for attenuation of clinical disease by an ERβ ligand. *Proc Natl Acad Sci USA* 110(47):19125–19130.
7. Saijo K, Collier JG, Li AC, Katzenellenbogen JA, Glass CK (2011) An ADIOL-ERβ-CtBP transrepression pathway negatively regulates microglia-mediated inflammation. *Cell* 145(4):584–595.
8. De Angelis M, Stossi F, Carlson KA, Katzenellenbogen BS, Katzenellenbogen JA (2005) Indazole estrogens: Highly selective ligands for the estrogen receptor beta. *J Med Chem* 48(4):1132–1144.
9. Crawford DK, Mangiardi M, Tiwari-Woodruff SK (2009) Assaying the functional effects of demyelination and remyelination: Revisiting field potential recordings. *J Neurosci Methods* 182(1):25–33.
10. Tiwari-Woodruff S, Morales LB, Lee R, Voskuhl RR (2007) Differential neuroprotective and antiinflammatory effects of estrogen receptor (ER)alpha and ERbeta ligand treatment. *Proc Natl Acad Sci USA* 104(37):14813–14818.
11. Zhang Y, et al. (1998) Estrogen-induced keratinocyte growth factor mRNA expression in normal and cancerous human breast cells. *Oncol Rep* 5(3):577–583.
12. Mannara F, et al. (2012) Passive experimental autoimmune encephalomyelitis in C57BL/6 with MOG: Evidence of involvement of B cells. *PLoS ONE* 7(12):e52361.
13. Mangiardi M, et al. (2011) An animal model of cortical and callosal pathology in multiple sclerosis. *Brain Pathol* 21(3):263–278.
14. Moore S, Patel R, Hannsun G, Yang J, Tiwari-Woodruff SK (2013) Sex chromosome complement influences functional callosal myelination. *Neuroscience* 245:166–178.
15. Ffrench-Constant C, Raff MC (1986) The oligodendrocyte-type-2 astrocyte cell lineage is specialized for myelination. *Nature* 323(6086):335–338.
16. Nait-Oumesmar B, Picard-Riéra N, Kerninon C, Baron-Van Evercooren A (2008) The role of SVZ-derived neural precursors in demyelinating diseases: From animal models to multiple sclerosis. *J Neurol Sci* 265(1-2):26–31.
17. Franklin RJ, Ffrench-Constant C (2008) Remyelination in the CNS: From biology to therapy. *Nat Rev Neurosci* 9(11):839–855.
18. Hisahara S, Yuan J, Momoi T, Okano H, Miura M (2001) Caspase-11 mediates oligodendrocyte cell death and pathogenesis of autoimmune-mediated demyelination. *J Exp Med* 193(1):111–122.
19. Narayanan SP, Flores AI, Wang F, Macklin WB (2009) Akt signals through the mammalian target of rapamycin pathway to regulate CNS myelination. *J Neurosci* 29(21):6860–6870.
20. Flores AI, et al. (2008) Constitutively active Akt induces enhanced myelination in the CNS. *J Neurosci* 28(28):7174–7183.
21. Bibollet-Bahena O, Almazan G (2009) IGF-1-stimulated protein synthesis in oligodendrocyte progenitors requires PI3K/mTOR/Akt and MEK/ERK pathways. *J Neurochem* 109(5):1440–1451.
22. Howell OW, et al. (2010) Activated microglia mediate axoglial disruption that contributes to axonal injury in multiple sclerosis. *J Neuropathol Exp Neurol* 69(10):1017–1033.
23. Trapp BD, Nave KA (2008) Multiple sclerosis: An immune or neurodegenerative disorder? *Annu Rev Neurosci* 31:247–269.
24. Papadopoulou A, et al. (2013) Contribution of cortical and white matter lesions to cognitive impairment in multiple sclerosis. *Mult Scler* 19(10):1290–1296.
25. Offner H, Adlard K, Zamora A, Vandenbark AA (2000) Estrogen potentiates treatment with T-cell receptor protein of female mice with experimental encephalomyelitis. *J Clin Invest* 105(10):1465–1472.
26. Sicotte NL, et al. (2002) Treatment of multiple sclerosis with the pregnancy hormone estriol. *Ann Neurol* 52(4):421–428.
27. Yarger JG, et al. (2013) Structurally similar estradiol analogs uniquely alter the regulation of intracellular signaling pathways. *J Mol Endocrinol* 50(1):43–57.
28. Lindberg MK, et al. (2003) Estrogen receptor (ER)-beta reduces ERalpha-regulated gene transcription, supporting a "ying yang" relationship between ERalpha and ERbeta in mice. *Mol Endocrinol* 17(2):203–208.
29. Boroojerdi B, Hungs M, Mull M, Töpper R, Noth J (1998) Interhemispheric inhibition in patients with multiple sclerosis. *Electroencephalogr Clin Neurophysiol* 109(3):230–237.
30. Ozturk A, et al. (2010) MRI of the corpus callosum in multiple sclerosis: Association with disability. *Mult Scler* 16(2):166–177.
31. Planey SL, Kumar R, Arnott JA (2014) Estrogen receptors (ERα versus ERβ): Friends or foes in human biology? *J Recept Signal Transduct Res* 34(1):1–5.
32. Wu WF, et al. (2013) Targeting estrogen receptor β in microglia and T cells to treat experimental autoimmune encephalomyelitis. *Proc Natl Acad Sci USA* 110(9):3543–3548.
33. Crawford DK, Mangiardi M, Xia X, López-Valdés HE, Tiwari-Woodruff SK (2009) Functional recovery of callosal axons following demyelination: A critical window. *Neuroscience* 164(4):1407–1421.
34. Moore S, Khalaj AJ, Yoon J, Patel R, Hannsun G, Yoo T, Sasidhar M, Martinez-Torres L, Hayardeny L, & Tiwari-Woodruff SK (2013) Therapeutic laquinimod treatment decreases inflammation, initiates axon remyelination, and improves motor deficit in a mouse model of multiple sclerosis. *Brain behav* 3, 664–682.
35. Franklin K, Paxinos G (2001) The Mouse Brain. *Stereotaxic Coordinates* (Academic Press, San Diego).